2023

Flow Patterns for Newtonian and Non-Newtonian Fluids in A Cylindrical Pipe

Erick Sanchez

Dambaru Bhatta

Applications and Applied Mathematics: An International Journal (AAM)

Volume 18 | Issue 1 Article 4

6-2023

(R2052) Flow Patterns for Newtonian and Non-Newtonian Fluids in a Cylindrical Pipe

Erick Sanchez
The University of Texas Rio Grande Valley

Dambaru Bhatta
The University of Texas Rio Grande Valley

Available at
http://pvamu.edu/aam
Appl. Appl. Math.
ISSN: 1932-9466

Applications and Applied Mathematics:
An International Journal
(AAM)

Vol. 18, Issue 1 (June 2023), Article 4, 11 pages

Flow Patterns for Newtonian and Non-Newtonian Fluids in A Cylindrical Pipe

Erick Sanchez and [1*]Dambaru Bhatta

School of Mathematical and Statistical Sciences
The University of Texas Rio Grande Valley
1201 West University Drive
Edinburg,Texas
[1]dambaru.bhatta@utrgv.edu

*Corresponding author

Received: November 16, 2022; Accepted: April 17, 2023

Abstract

A fully developed laminar steady flow of an incompressible, viscous fluid in a horizontal cylindrical pipe is considered here. Flow patterns for an incompressible, viscous fluid for both Newtonian and non-Newtonian fluids such as shear-thinning, shear-thickening and Bingham plastic fluids are analyzed in this study. Assuming that the flow is only due to the wall shear stress and the pressure drop, the velocity component in the axial direction for these cases is derived. Computational results of the velocity profiles for various cases are obtained using MATLAB and presented in graphical forms. It is observed that the velocity profile is parabolic for Newtonian fluid whereas it is flatter for a shear-thinning fluid and sharper for a shear-thickening fluid. For a Bingham fluid, the velocity reaches a constant value known as the plug velocity in the central plug flow region, and it decreases gradually to zero at the pipe wall.

Keywords: Newtonian; non-Newtonian; Incompressible; Viscous; Shear-thinning; Shear-thickening

MSC 2010 No.: 35Q35, 76A02, 76A05, 97M10

1. Introduction

Sir Isaac Newton is universally recognized for key developments in various fields, especially mathematics, astronomy, and physics including the derivation of the laws of motion and universal gravitation. Through these laws, Newton studied the way fluids behave by observing their various properties such as viscosity, density and temperature. He discovered that behavior of most fluids changes with variations in temperature or pressure. However, this does not apply to every fluid. A fluid is considered to be compressible if its density varies and is considered to be incompressible if its density is treated as constant. There exist some fluids in which one cannot find a linear relationship between the stress applied to the fluid and the rate at which the fluid distorts. These fluids are referred as non-Newtonian fluids. There are several different forms of non-Newtonian fluids, some of the important ones include shear-thinning, shear thickening and Bingham plastics.

Stress is the ratio of the amount of force applied to an object to its cross-sectional area. Larger objects are capable to resist higher forces. Strain indicates how much an object distorts when forces are applied to it. Most of the time, this distortion either causes the object to extend or compress, depending on how forces are applied. Strain is computed as the ratio of the change in length to the original length of the object. There are two main different types of deformation: elastic and plastic. Elastic distortion arises when stress is applied to an object and the distortion inevitably reverses itself when the external forces are detached. Plastic distortion is a permanent distortion. An object begins experiencing elastic deformation at first, but once the stress on the object surpasses a certain amount, it experiences plastic deformation. When that change happens, the object has reached its yield stress. Elastic deformation is linear. Plastic deformation is not linear, making it more demanding to model. In material science and engineering, the yield point is the point on a stress-strain curve that suggests the end of elastic behavior and the beginning of plastic behavior. Newton discovered that the viscosity of most fluids is affected by temperature or pressure. Newtonian fluid is defined by a linear relationship between the shear stress and the shear rate. The fluids such as water and oil are also considered to be Newtonian. Unlike Newtonian fluids, the viscosity of some fluids is affected by factors other than temperature. These fluids are referred as non-Newtonian fluids. Polymers are non-Newtonian fluids. When it comes to non-Newtonian fluids, shear stress and the shear rate follow a non-linear relationship. In non-Newtonian fluids, viscosity can either increase or decrease if a sheer stress is applied to it, i.e., it can either become more solid or more liquid depending on the type of non-Newtonian fluid. Non-Newtonian fluids are divided into various categories including shear-thinning, shear-thickening and Bingham plastics.

Classification, properties, and examples of various non-Newtonian fluids were discussed by different authors (Alderman, 1997; Chhabra et al., 2008). Bingham plastic fluid flow development was discussed by Florides et al. (2000). Computation of isothermal waxy crude oil flows was presented by Vinay et al. (2007). Analysis on non-Newtonian Fluid flow in Porous Media was carried by Shenoy (1994), Sochi (2010). Jeng et al. (2010) performed numerical simulation of Taylor Couette flow of Bingham fluids. A study on the steady flow and heat transfer of power-law fluids around a heated inclined square cylinder in a plane channel was presented by Aboueian-Jahromi et al. (2011). Time independent natural convection of non-Newtonian power-law fluid in a trapezoidal enclosure was analyzed by Sojoudi et al. (2013). Nirmalkar et al. (2014) studied momentum and heat transfer on a heated circular cylinder filled with Bingham plastic fluids. Heat transfer characteristics of power-law fluids over a semicircular cylinder were presented by Tiwari et al. (2015). Doludenko et al. (2016) studied the Rayleigh-Taylor instability of Newtonian and non-Newtonian fluids. Treating blood as non-Newtonian fluid, various authors studied blood flow through artery. Effects of the slip velocity and the shape of the stenosis on non-Newtonian flow of blood were analyzed numerically by Singh et al. (2015). Siddiqui et al. (2017) carried out mathematical analysis on pulsatile flow through a catheterized stenosed artery.

Here we consider an incompressible, viscous fluid in a horizontal cylindrical pipe. Assuming that the flow is due to the pressure drop and wall shear stress only, we derive the velocity component in the axial direction for Newtonian and non-Newtonian fluids such as power-law fluid and Bingham plastic fluid. Computational results for both type of fluids are presented.

2. Mathematical Derivations

We consider a fully developed steady laminar flow of an incompressible and viscous fluid in a horizontal cylindrical pipe. We assume that the flow is due to the pressure drop in the axial direction and wall shear stress. An elemental volume of ring shape of radial thickness $\triangle r$ and length $\triangle z$ and situated at a distance r for the axial z-direction as shown in Figure 1.

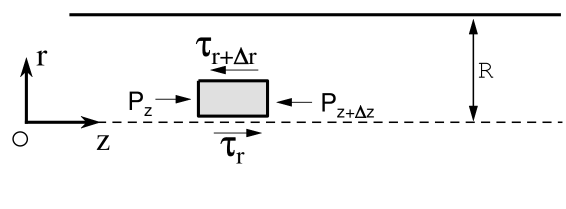

Figure 1. Cross section of an elemental volume inside a pipe

The radius of the cylinder is R. There is no motion in the radial direction and the motion in axial direction only. Let the velocity be denoted by $v(r)$. Considering the momentum balance for pressure and viscous forces, we have

$$(2\pi r \triangle z \, \tau)_r - (2\pi r \triangle r \, \tau)_{r+\triangle r} + (2\pi r \triangle r \, P)_z - (2\pi r \triangle r \, P)_{z+\triangle z} = 0,$$

which yields

$$2\pi \, (r \, \tau)_r \triangle z - 2\pi \, (r \, \tau)_{r+\triangle r} \triangle z + 2\pi r \, (P)_z \triangle r - 2\pi r \, (P)_{z+\triangle z} \triangle r = 0.$$

So, we get

$$\frac{(r \, \tau)_{r+\triangle r} - (r \, \tau)_r}{\triangle r} + r \, \frac{(P)_{z+\triangle z} - (P)_z}{\triangle z} = 0,$$

and in the limit as $\triangle r \to 0$, $\triangle z \to 0$. Finally, we obtain

$$\frac{d}{dr}(r\,\tau) + r\,\frac{dP}{dz} = 0. \tag{1}$$

Since the flow is in the positive z-direction due to pressure gradient and the pressure is decreasing from left to right of the cylinder, we take $\frac{dP}{dz} = -K$ where K is a positive constant. Now, integrating $\frac{d}{dr}(r\,\tau) = rK$ with respect to r, and assuming τ is finite at $r = 0$, we have

$$\tau(r) = \frac{rK}{2}. \tag{2}$$

Result given in (2) can be used to obtain the velocity profile $v(r)$.

2.1. Velocity Profile for Newtonian Fluid

Here, we consider the flow of a Newtonian fluid through the cylinder. For a Newtonian fluid, we have $\tau = -\mu\frac{dv}{dr}$. Using this in Equation (2) and integrating with respect to r, we have

$$v(r) = -\frac{r^2K}{4\mu} + C_2,$$

where C_2 is a constant of integration. Using the zero velocity, $v(R) = 0$, at the cylinder boundary, finally, we can express $v(r)$ as

$$v(r) = \frac{R^2K}{4\mu} - \frac{r^2K}{4\mu} = \frac{K}{4\mu}\left(R^2 - r^2\right).$$

Using the notation, v_0, for velocity at the center, i.e., at $r = 0$, we get $v_0 = \frac{R^2K}{4\mu}$. Hence, we obtain the velocity profile for Newtonian fluid as

$$v(r) = v_0\left[1 - \left(\frac{r}{R}\right)^2\right], \quad \text{where} \quad v_0 = \frac{R^2K}{4\mu}. \tag{3}$$

2.2. Velocity Profile for Non-Newtonian fluids

Here, we consider the flow of two non-Newtonian fluids through a horizontal cylinder: (i) Power Law Fluid and (ii) Bingham Fluid. Figure 2(a) presents a relationship of shear rate versus shear stress and Figure 2(b) displays a relationship of shear rate versus viscosity for Newtonian, shear thinning and shear thickening fluids.

2.2.1. *Power Law Fluid*

For power law fluid, we can have $\tau = -\eta\frac{dv}{dr}$ where $\eta = \mu\left|\frac{dv}{dr}\right|^{n-1}$. For Newtonian, $n = 1$, which yields $\eta = \mu$. Using (2) in power law fluid, we have

$$\frac{dv}{dr} = -\left[\frac{rK}{2\mu}\right]^{1/n}.$$

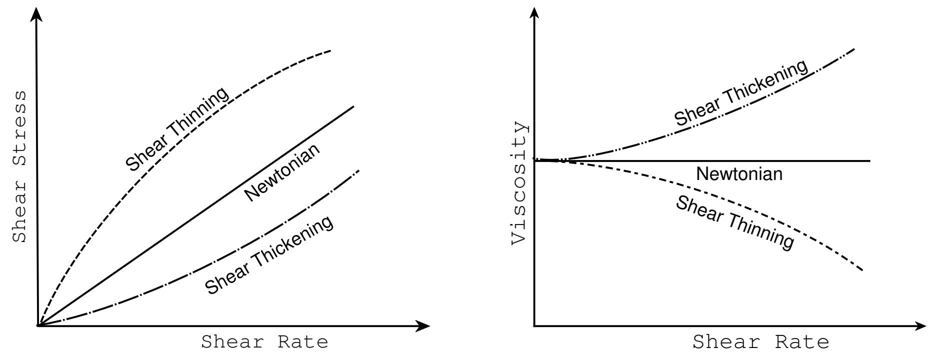

Figure 2. (a) Shear Rate vs Stress and (b) Shear Rate vs Viscosity Graphs

Integrating with respect to r, we get

$$v(r) = -\left[\frac{K}{2\mu}\right]^{1/n} \times \frac{r^{1+1/n}}{1+1/n} + C_3,$$

where C_3 is a constant of integration. Using the zero velocity, $v(R) = 0$, at the cylinder boundary, $C_3 = \left[\frac{K}{2\mu}\right]^{1/n} \times \frac{R^{1+1/n}}{1+1/n}$.

Thus, finally we can express $v(r)$ as

$$\begin{aligned} v(r) &= \left[\frac{K}{2\mu}\right]^{1/n} \times \frac{R^{1+1/n}}{1+1/n} - \left[\frac{K}{2\mu}\right]^{1/n} \times \frac{r^{1+1/n}}{1+1/n} \\ &= \frac{n}{n+1}\left[\frac{K}{2\mu}\right]^{1/n}\left(R^{1+1/n} - r^{1+1/n}\right). \end{aligned}$$

Using the notation v_0 for velocity at the center, i.e., at $r = 0$, we get $v_0 = \frac{n}{n+1}\left[\frac{K}{2\mu}\right]^{1/n} R^{1+1/n}$. Hence, we get the velocity profile as

$$v(r) = v_0\left[1 - \left(\frac{r}{R}\right)^{1+1/n}\right], \quad \text{where} \quad v_0 = \frac{nR^{1+1/n}}{n+1}\left[\frac{K}{2\mu}\right]^{1/n}. \tag{4}$$

2.2.2. *Bingham Fluid*

For Bingham Fluid, shear stress τ is defined as

$$\tau = \tau_y - \mu\frac{dv}{dr} \qquad \text{for} \qquad \frac{dv}{dr} \neq 0,\ r_b < r \leq R, \tag{5}$$

$$\tau \leq \tau_y \qquad \text{for} \qquad \frac{dv}{dr} = 0,\ 0 \leq r \leq r_b, \tag{6}$$

where τ_y and μ denote the yield stress and viscosity, respectively.

For Newtonian, $\tau_y = 0$. This implies that inside a cylindrical surface of radius r_b the material flows like solid plug. Now (2) and (5) yield us

$$\frac{dv}{dr} = \frac{\tau_y}{\mu} - \frac{rK}{2\mu}. \tag{7}$$

Integrating (7) with respect to r, for $r_b \leq r \leq R$, using no slip velocity condition $v(R) = 0$ at the cylinder boundary, we obtain $v(r)$ as

$$\begin{aligned} v(r) &= \frac{K}{4\mu}\left[R^2 - r^2\right] - \frac{\tau_y}{\mu}\left[R - r\right] \\ &= \frac{KR^2}{4\mu}\left[1 - \left(\frac{r}{R}\right)^2\right] - \frac{\tau_y R}{\mu}\left[1 - \frac{r}{R}\right]. \end{aligned} \tag{8}$$

When $\tau_y = 0$, we obtain the results same as Newtonian fluid

$$v(r) = \frac{KR^2}{4\mu}\left[1 - \left(\frac{r}{R}\right)^2\right]. \tag{9}$$

Using the notation v_b for velocity for the solid plug in the region $r \leq r_b$, i.e., putting $r = r_b$ in (8), we get

$$\begin{aligned} v_b &= \frac{KR^2}{4\mu}\left[1 - \left(\frac{r_b}{R}\right)^2\right] - \frac{\tau_y R}{\mu}\left[1 - \frac{r_b}{R}\right] \\ &= \frac{KR^2}{4\mu}\left[1 - \left(\frac{r_b}{R}\right)^2 - \frac{2r_b}{R}\left(1 - \frac{r_b}{R}\right)\right] \\ &= \frac{KR^2}{4\mu}\left(1 - \frac{r_b}{R}\right)^2, \end{aligned}$$

and, finally

$$v_b = \frac{KR^2}{4\mu}\left(1 - \frac{2\tau_y}{KR}\right)^2, \quad 0 \leq r \leq r_b. \tag{10}$$

3. Results and Discussion

Here, we present the velocity component, $v(r)$, for Newtonian and for two kinds of non-Newtonian fluids, namely, power law and Bingham fluids for different parameters. Computed results of the equations (3), (4), (8) and (10) follow.

3.1. Newtonian Fluid

Results for the velocity component for various μ for a fixed value of $K = 0.6$ are shown in Figure 3 for Newtonian fluid. It is observed that the velocity profile is parabolic and having maximum along the axis of the cylinder and reaching zero value at the surface of the cylinder. It is clear that as viscosity increases, the velocity decreases.

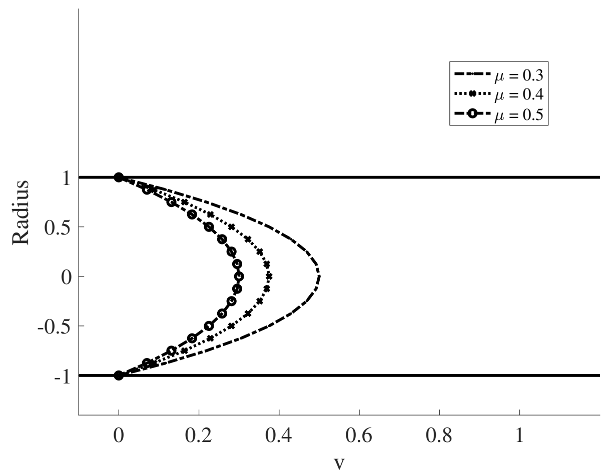

Figure 3. Velocity for Newtonian fluid for various μ

Figure 4 is used to display results for the velocity component of Newtonian fluid for various K at a fixed value of viscosity $\mu = 0.4$. It is observed that the the axial velocity is increasing if the pressure difference is increasing. The rate of change in velocity component is higher for higher pressure difference.

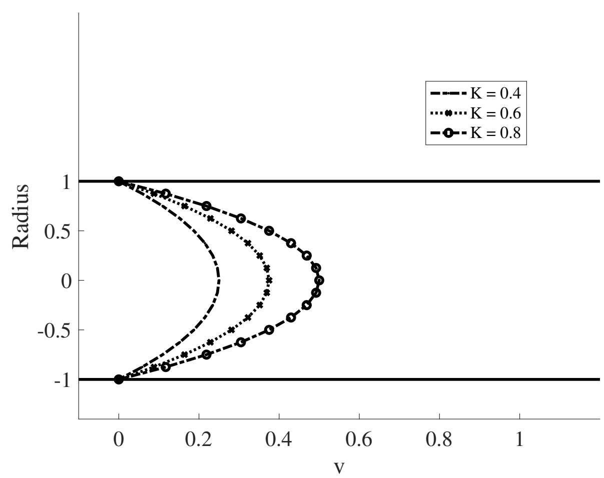

Figure 4. Velocity for Newtonian fluid for various K

3.2. Non-Newtonian Power Law Fluid

In this section, we present behavior of velocity of non-Newtonian fluid which obey power law. First we consider the effect of pressure variation on the flow. Results for the velocity component with varying pressure gradient, K, with fixed $\mu = 0.4$ and $n = 0.4$ are shown in Figure 5 for power law fluid. The axial velocity decreases if the pressure difference decreases. The velocity profile is constant (flat, zero rate of change) at a central band (plug region) whereas for Newtonian fluid it always increases towards the center of the pipe. Also the band of the flatness becomes larger for smaller values of K.

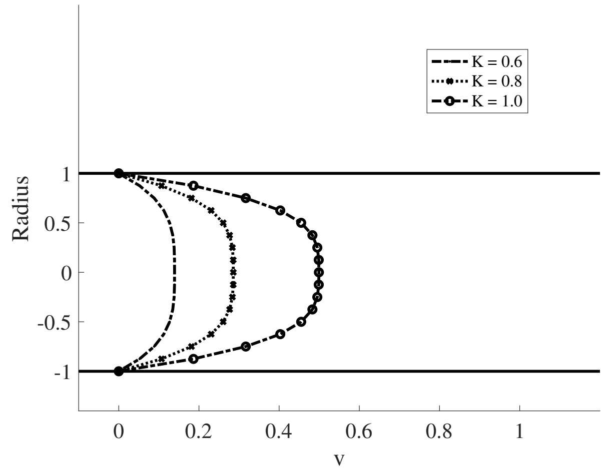

Figure 5. Velocity for power law fluid for various K

Figure 6 is used to display results for the velocity component of power law fluid for various μ when $K = 0.8$ and $n = 0.4$. The axial velocity increases if μ decreases and its rate of change is zero at a central plug region.

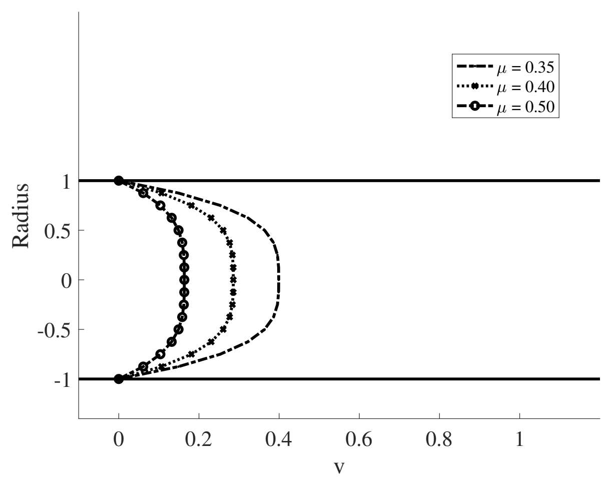

Figure 6. Velocity for power law fluid for various μ

The velocity component for various n is displayed in Figure 7 for power law fluid with $K = 0.8$ and $\mu = 0.4$. The velocity profile is constant (rate of change is zero) at a central plug region for $n < 1$. The velocity profile is sharper at the center for $n > 1$ than the Newtonian fluid when $n = 1$.

3.3. Non-Newtonian Bingham Fluid

Results for the velocity component for various pressure gradient, K, are shown in Figure 8 for Bingham fluid with $\mu = 0.3$ and $\tau_y = 0.15$. The axial velocity increases as K increases and its rate

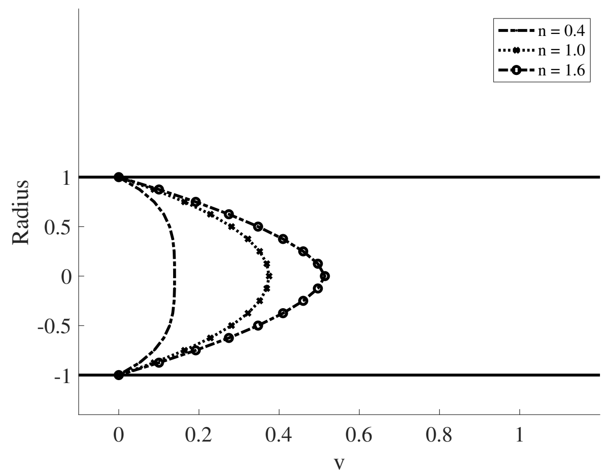

Figure 7. Velocity for power law fluid for various n

of change is zero at a central band (plug region) and the width of the band increases as pressure gradient decreases.

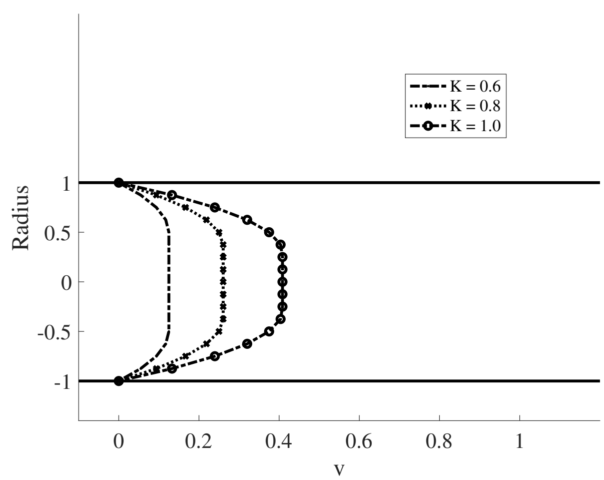

Figure 8. Velocity for Bingham fluid for various K

Figure 9 is used to depict the results for the velocity component for various μ for Bingham fluid with $K = 0.8$ and $\tau_y = 0.15$. The axial velocity decreases as μ increases and its rate of change is zero at a central plug region.

Results for the velocity component for various τ_y for Bingham fluid are displayed in Figure 10 with $K = 0.8$ and $\mu = 0.4$. As the yield stress, τ_y, is increasing, the axial velocity is decreasing. The velocity profile is constant, i.e., the rate of change is zero at a central band (plug region) and the width of the band increases as τ_y increases. When yield stress reduces to zero, velocity profile displays the behavior of a Newtonian fluid.

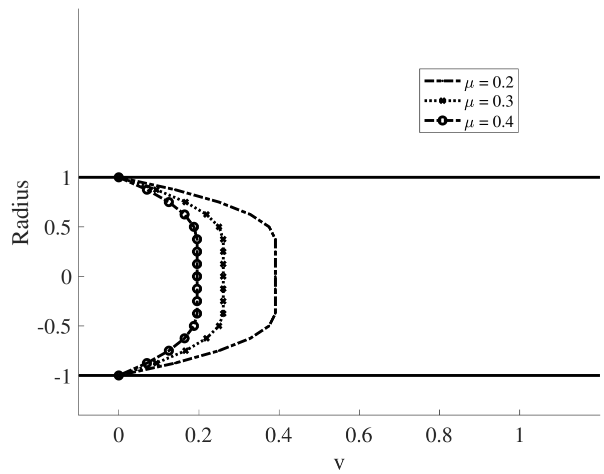

Figure 9. Velocity for Bingham fluid for various μ

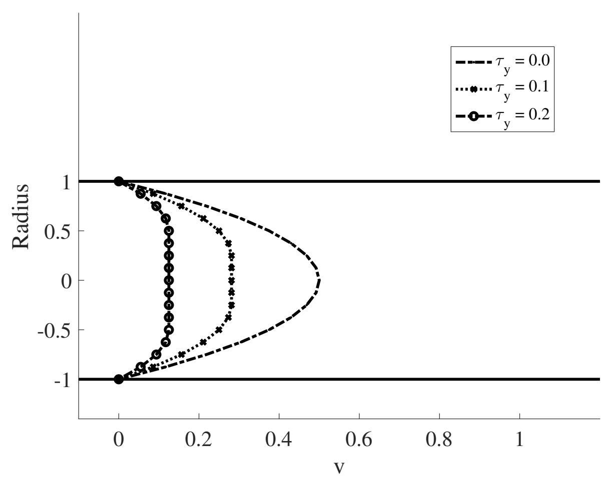

Figure 10. Velocity for Bingham fluid for various τ_y

4. Conclusion

Here, flow patterns for both Newtonian and non-Newtonian fluids such as shear-thinning, shear-thickening and Bingham plastic fluids in a cylindrical pipe are analyzed. We assume that fluid is incompressible and viscous. We obtain velocity profile for both Newtonian fluid and non-Newtonian fluids, specifically shear-thinning, shear-thickening and Bingham plastic fluids. Assuming that the flow is due to the pressure drop and wall shear stress only, we derived the expressions for the velocity component in the axial direction for these cases. Computational results of the velocity profiles for various scenarios have been presented. It has been observed that velocity profile is parabolic for Newtonian fluid whereas it is flatter for a shear-thinning and sharper for a shear-thickening fluid. For a Bingham fluid, the velocity reaches a constant value known as the plug velocity in the central plug flow region and it decreases gradually to zero at the pipe wall. The velocity profile is constant (rate of change is zero) at a central plug region. The width of the plug region increases with increasing yield stress as well as with decreasing pressure gradient.

Acknowledgment:

Authors would like to thank the referees for their constructive suggestions to improve the quality of the paper.

REFERENCES

Aboueian-Jahromi, J., Nezhad, A.H. and Behzadmehr, A. (2011). Effects of inclination angle on the steady flow and heat transfer of power-law fluids around a heated inclined square cylinder in a plane channel, Journal of Non-Newtonian Fluid Mechanics, Vol. 166, pp. 1406-1414.

Alderman, N. (1997). *Non-Newtonian Fluids: Guide to Classification and Characteristics*.

Chhabra, R.P. and Richardson, J.F. (2008). *Non-Newtonian Flow and Applied Rheology*, Second Edition, Butterworth-Heinemann/Elsevier.

Doludenko, A.N., Fortova, S.V. and Son, E.E. (2016). The Rayleigh-Taylor instability of Newtonian and non-Newtonian fluids, Physica Scripta, Vol. 91, pp. 1-9.

Florides, G.C., Alexandrou, A.N., Georgios, C. and Georgiou, G.C. (2000). Flow development in compression of a finite amount of a Bingham plastic, Journal of Non-Newtonian Fluid Mechanics, Vol. 143, No. 1, pp. 38-47.

Jeng, J. and Zhu, K.Q. (2010). Numerical simulation of Taylor Couette flow of Bingham fluids, Journal of Non-Newtonian Fluid Mechanics, Vol. 165, pp. 1161-1170.

Nirmalkar, N. and Chhabra, R.P. (2014). Momentum and heat transfer from a heated circular cylinder in Bingham plastic fluids, Int. J. Heat Mass Transf. , Vol. 90, pp. 564-577.

Shenoy, A.V. (1994). Non-Newtonian fluid and heat transfer in porous media Advances in Heat Transfer, Vol. 24, pp. 101-190

Siddiqui, S.U. and Awasthi, C. (2017). Mathematical analysis on pulsatile flow through a catheterized stenosed artery, Journal of Applied Mathematics and Physics, Vol. 5, pp. 1874-1886.

Singh, A., Shrivastav, R.K. and Bhatnagar, A. (2015). A numerical analysis for the effect of slip velocity and stenosis shape on non-newtonian flow of blood, International Journal of Engineering, Vol. 28, No. 3, pp. 440-446.

Sochi, T. (2010). Flow of non-Newtonian fluids in porous media, Journal of Polymer Science, Vol. 48, pp. 2437-2767.

Sojoudi, A., Saha, S.C., Gu, Y.T. and Hossain, M.A. (2013). Steady natural convection of non-Newtonian power-law fluid in a trapezoidal enclosure, Adv. Mech. Eng., Vol. 5, pp. 1-8.

Tiwari, A.K. and Chhabra, R.P. (2015). Momentum and heat transfer characteristics for the flow of power-law fluids over a semicircular cylinder, Numerical Heat Transfer, Vol. 66, No. 12, pp. 1365-1388.

Vinay, G., Wachs, A. and Frigaard, I.J. (2007). Start-up transients and efficient computation of isothermal waxy crude oil flows, J. Nonnewton. Fluid Mech., Vol. 143, pp. 141-156.